

Structure-Based Design of a Novel, Potent, and Selective Inhibitor for MMP-13 Utilizing NMR Spectroscopy and Computer-Aided Molecular Design

James M. Chen,^{*,‡} Frances C. Nelson,[†] Jeremy I. Levin,[†] Dominick Mobilio,[†] Franklin J. Moy, Ramaswamy Nilakantan, Arie Zask,[†] and Robert Powers^{*}

Contribution from the Department of Biological Chemistry, Wyeth Research, 85 Bolton St., Cambridge, Massachusetts 02140 and the Department of Chemical Sciences, Wyeth Research, 401 N. Middletown Rd., Pearl River, NY 10965

Received May 4, 2000. Revised Manuscript Received July 12, 2000

Abstract: The high-resolution NMR solution structure of the catalytic fragment of human collagenase-3 (MMP-13) was used as a starting point for structure-based design of selective inhibitors for MMP-13. The major structural difference observed between the MMP structures is the relative size and shape of the S1' pocket where this pocket is significantly longer for MMP-13, nearly reaching the surface of the protein. On the basis of the extended nature of the MMP-13 S1' pocket an inhibitor potent and selective for MMP-13 was designed from an initial high throughput screening (HTS) lead. CL-82198 was identified as a weak (10 μ M) inhibitor against MMP-13 while demonstrating no activity against MMP-1, MMP-9, or the related enzyme TACE. The drug-like properties of CL-82198 made it an ideal candidate for optimization of enzyme potency and selectivity. On the basis of NMR binding studies, it was shown that inhibitor CL-82198 bound within the entire S1' pocket of MMP-13 which is the basis of its selectivity against MMP-1, MMP-9, and TACE. A strategy utilizing this information was devised for designing new inhibitors that showed enhanced selectivity toward MMP-13. Our design strategy combined the critical selectivity features of CL-82198 with the known potency features of a nonspecific MMP inhibitor (WAY-152177) to generate a potent and selective MMP-13 inhibitor (WAY-170523). WAY-170523 has an IC₅₀ of 17 nM for MMP-13 and showed >5800-, 56-, and >500-fold selectivity against MMP-1, MMP-9, and TACE, respectively.

A structure-based approach to designing potent and selective inhibitors has established itself as an important component of the drug development process (for reviews see refs 1 and 2). This is evident by the extensive structural data available for the matrix metalloproteinase (MMP) family of enzymes and the emergence of unique inhibitors based on this structural information (for reviews see refs 3–7). The MMPs are involved in the degradation of the extracellular matrix that is associated with normal tissue remodeling processes such as pregnancy, wound healing, and angiogenesis. MMP expression and activity is highly controlled because of the degradative nature of these enzymes where the apparent loss in this regulation results in the pathological destruction of connective tissue and the ensuing disease state. Thus, the MMPs are a highly active set of targets for the design of therapeutic agents for the disease areas of arthritis and oncology. The MMP family is composed of a number of enzymes where MMP-13 was recently identified on

the basis of differential expression in normal breast tissues and in breast carcinoma. Recently, both an NMR and X-ray structure of inhibited MMP-13 have been reported.^{8,9}

The MMPs are generally categorized based on their substrate specificity, where the collagenase subfamily of MMP-1, MMP-8, and MMP-13 selectively cleaves native interstitial collagens (types I, II, and III). It is likely that only a subset of MMP enzymes will be involved in a particular disease as is evident by the overexpression of MMP-13 in breast carcinoma and MMP-1 in papillary carcinomas. Therefore, the current paradigm in the development of MMP inhibitors is to design specificity into the structures of the small molecules based on the postulation that a broad-spectrum MMP inhibitor would provide a higher exposure to toxic side effects.

Nevertheless, there is a close similarity in the overall three-dimensional fold for the MMP family of proteins, which is consistent with the relatively high sequence homology (>40%), making the design of a selective MMP inhibitor a nontrivial task. The concept of designing selective MMP inhibitors has been facilitated by the extensive structural data available for the MMPs where a significant difference in the size and shape of the S1' pocket has been observed.^{8–26} This structural

* Address correspondence to these authors at the Department of Biological Chemistry.

[†] Department of Chemical Sciences.

[‡] Current address: Tularik Inc., Two Corporate Dr., South San Francisco, CA 94010. Phone: (650)-825-7458. E-mail: jchen@tularik.com.

(1) Gubernator, K.; Boehm, H. J. *Methods Princ. Med. Chem* **1998**, *6*, 15–36.

(2) Kubinyi, H. *Curr. Opin. Drug Discovery Dev.* **1998**, *1*, 4–15.

(3) Woessner, J. F., Jr. *FASEB J.* **1991**, *5*, 2145–54.

(4) Ries, C.; Petrides, E. *Biol. Chem. Hoppe-Seyler* **1995**, *376*, 345–55.

(5) Browner, M. F. *Perspect. Drug Discovery Des.* **1995**, *2*, 343–51.

(6) Morphy, J. R.; Millican, T. A.; Porter, J. R. *Curr. Med. Chem.* **1995**, *2*, 743–62.

(7) Zask, A.; Levin, J. I.; Killar, L. M.; Skotnicki, J. S. *Curr. Pharm. Des.* **1996**, *2*, 624–661.

(8) Lovejoy, B.; Welch, A. R.; Carr, S.; Luong, C.; Broka, C.; Hendricks, R. T.; Campbell, J. A.; Walker, K. A. M.; Martin, R.; Van Wart, H.; Browner, M. F. *Nat. Struct. Biol.* **1999**, *6*, 217–221.

(9) Moy, F. J.; Chanda, P., K.; Chen, J., M.; Cosmi, S.; Edris, W.; Levin, J. I.; Wilhelm, J.; Powers, R. *J. Mol. Biol.* **2000**, *302*, 673–691.

(10) Bode, W.; Reinemer, P.; Huber, R.; Kleine, T.; Schnierer, S.; Tschesche, H. *EMBO J.* **1994**, *13*, 1263–9.

(11) Gooley, P. R.; O'Connell, J. F.; Marcy, A. I. *Nat. Struct. Biol.* **1994**, *1*, 111–18.

difference across the MMP family provides an obvious approach for designing specificity into potent MMP inhibitors by designing compounds that appropriately fill the available space in the S1' pocket while taking advantage of sequence differences. A number of examples have been previously reported using this approach where some selectivity between MMPs has been achieved by incorporating a biphenyl into the S1' pocket.^{8,27,28} The recent NMR and X-ray structures for MMP-13 indicated an unusually large S1' pocket for MMP-13 suggesting that it may be feasible to take advantage of this feature to design a selective MMP-13 inhibitor.^{8,9} Here we report a novel, potent inhibitor highly selective for MMP-13 that has been identified by optimizing an initial lead from high throughput screening based on an NMR structure of its complex with MMP-13 in conjunction with computer aided molecular design.

Experimental Methods

High Throughput Screening Analysis. A total of 58079 compounds were analyzed for MMP-13 inhibitor activity in a high throughput screen (HTS). Enzyme activity was assessed using nonlabeled recombinant MMP-13 and a peptide substrate.^{29,30} MMP-13 activity was determined using 50 mM HEPES buffer with 5 mM CaCl₂, 0.02% Brij 35 (polyoxyethylene 23 lauryl ether), and 0.5% Cysteine at pH 7.0. The HTS was a kinetic assay where compounds were screened at a concentration of 10 µg/mL with final MMP-13 and DMSO concentrations of 5 nM and <1.0%, respectively. A total of 385 compounds were identified that inhibited ≥40% of MMP-13 activity. From the 385 actives, 162 structures were eliminated by visual inspection using considerations such as synthetic accessibility and reactivity. The remaining 223 active compounds were clustered (using the Jarvis–

Patrick method) into related sets of structures.³¹ The active structures were analyzed by their calculated physical properties (total number of non-hydrogen atoms, number of heteroatoms, number of hydrogen-bond donors, number of hydrogen-bond acceptors, calculated log P, molecular weight) as well as known cytotoxicity as measured by the 3-(4,5-dimethylthiazol-2-yl)-2,5-diphenyl tetrazolium bromide, when available.

The properties of each compound were normalized against a set of known orally bioavailable drugs.³³ Specifically, the mean and standard deviation of the six calculated properties were determined for the set of orally bioavailable drugs. Then, for each assayed compound, the normalized property value was obtained by subtracting the mean value and dividing by the standard deviation for the known drugs. The normalized property profiles for each structure in a cluster were plotted side by side as a column graph to obtain the cluster's profile, clusters containing a high percentage of cytotoxic compounds (as measured by the MTT assay described above) would be eliminated from further consideration. Similarly, any significant deviation from the profiles of the orally bioavailable drugs would also eliminate the cluster from further analysis.

Synthesis of WAY-170523. General: Melting points were obtained on a Mel-Temp apparatus and are uncorrected. ¹H spectra were recorded at 75, 100, 300, or 400 MHz as indicated and are expressed in δ (ppm) with TMS as an internal standard. Infrared spectra were recorded as a KBr press on a Niclete 710. Low-resolution mass spectra were determined on a Micromass platform electrospray ionization quadrupole mass spectrometer. High-resolution mass spectra were determined on a Bruker 9.4 T FTMS. Elemental analyses were performed on a Perkin-Elmer Series II CHNS/O Analyzer and are within 0.4% of theory. Thin-layer chromatography was performed on silica gel 60 F-254 (EM Reagents). Flash column chromatography was carried out using silica gel 60 (230–400 mesh). Solvents and reagents were obtained from commercial sources and used without additional purification. All chemical yields are not optimized and generally represent the result of a single experiment.

Benzofuran-2-carboxylic acid (2-hydroxyethyl)amide (11): To a solution of 2-benzofurancarboxylic acid (1.0 g, 6.16 mmol), 1-(3-dimethylaminopropyl)-3-ethylcarbodiimide hydrochloride (1.0 g, 6.16 mmol), and 1-hydroxybenzotriazole (1.08 g, 8.0 mmol) in DMF (12 mL) at 0 °C was added ethanollamine (0.37 mL, 6.16 mmol) and 4-methylmorpholine (2.04 mL, 9.24 mmol). The reaction was stirred at 0 °C for an additional 10 min and then warmed to room temperature and stirred for 4 h. The reaction mixture was then diluted with ethyl acetate, washed three times with H₂O, once with NaHCO₃ (saturated), and once with brine, dried over MgSO₄, and concentrated in vacuo to provide 0.55 g (43% yield) of the desired product as a pale yellow solid. Mp 90–91 °C. IR (KBr) 3349, 3256, 1614, 1597, 1539, 1302, 1182, 1069, 743 cm⁻¹. ¹H NMR (300 MHz, DMSO-*d*₆) δ 3.43 (dq, *J* = 5.85, 52.0 Hz, 5 H), 4.78 (t, *J* = 5.60 Hz, 1 H), 7.33 (m, 1 H), 7.46 (m, 1 H), 7.53 (d, *J* = 0.84 Hz, 1 H), 7.65 (dd, *J* = 0.66, 8.56 Hz, 1 H), 7.73 (d, *J* = 18.69 Hz, 1 H), 8.63, (t, *J* = 5.70 Hz). ¹³C NMR (75 MHz, DMSO-*d*₆) δ 41.93, 59.89, 109.57, 112.08, 123.06, 124.0, 127.07, 127.51, 149.58, 154.49, 158.53. Electrospray mass spec: *m/z* 205.8 [(M + H)⁺ C₁₁H₁₂NO₃ requires 206.07]. Anal. Calcd for C₁₁H₁₁NO₃: C, 64.38; H, 5.40; N, 6.83. Found: C, 64.20; H, 5.30; N, 6.84.

2-[[4-{2-[(1-Benzofuran-2-ylcarbonyl)amino]ethoxy}phenyl)sulfonyl](benzyl)amino]-3,5-dimethylbenzoic acid (13): Benzofuran-2-carboxylic acid (2-hydroxyethyl)amide (157 mg, 0.76 mmol) was dissolved in DMF (1.5 mL) and cooled to 0 °C. Sodium hydride (76 mg, 1.9 mmol) was added and the reaction was stirred for 30 min. To this solution was added acid **12** (289 mg, 0.73 mmol) in DMF (2 mL). The reaction was held at 0 °C for an additional 30 min and then allowed to warm to room temperature and stirred overnight. The reaction was then quenched with 1 M HCl and extracted three times with CH₂Cl₂.

(12) Lovejoy, B.; Cleasby, A.; Hassell, A. M. *Ann. N.Y. Acad. Sci.* **1994**, *732*, 375–8.

(13) Lovejoy, B.; Hassell, A. M.; Luther, M. A. *Biochemistry* **1994**, *33*, 8207–17.

(14) Lovejoy, B.; Cleasby, A.; Hassell, A. M. *Science* **1994**, *263*, 375–7.

(15) Spurlino, J. C.; Smallwood, A. M.; Carlton, D. D.; Banks, T. M.; Vavra, K. J.; Johnson, J. S.; Cook, E. R.; Falvo, J.; Wahl, R. C.; et al. *Proteins: Struct., Funct., Genet.* **1994**, *19*, 98–109.

(16) Stams, T.; Spurlino, J. C.; Smith, D. L.; Wahl, R. C.; Ho, T. F.; Qoronfleh, M. W.; Banks, T. M.; Rubin, B. *Nat. Struct. Biol.* **1994**, *1*, 119–123.

(17) Becker, J. W.; Marcy, A. I.; Rokosz, L. L. *Protein Sci.* **1995**, *4*, 1966–76.

(18) Gonnella, N. C.; Bohacek, R.; Zhang, X.; Kolossvary, I.; Paris, C. G.; Melton, R.; Winter, C.; Hu, S.-I.; Ganu, V. *Proc. Natl. Acad. Sci. U.S.A.* **1995**, *92*, 462–6.

(19) Van Doren, S. R.; Kurochkin, A. V.; Hu, W.; Ye, Q.-Z.; Johnson, L. L.; Hupe, D. J.; Zuiderweg, E. R. P. *Protein Sci.* **1995**, *4*, 2487–2498.

(20) Botos, I.; Scapozza, L.; Zhang, D.; Liotta, L. A.; Meyer, E. F. *Proc. Natl. Acad. Sci. U.S.A.* **1996**, *93*, 2749–2754.

(21) Broutin, I.; Arnoux, B.; Riche, C.; Lecroisey, A.; Keil, B.; Pascard, C.; Ducruix, A. *Acta Crystallogr., Sect. D: Biol. Crystallogr.* **1996**, *D52*, 380–92.

(22) Gooley, P. R.; O'Connell, J. F.; Marcy, A. I.; Cuca, G. C.; Axel, M. G.; Caldwell, C. G.; Hagmann, W. K.; Becker, J. W. *J. Biomol. NMR* **1996**, *7*, 8–28.

(23) Betz, M.; Huxley, P.; Davies, S. J.; Mushtaq, Y.; Pieper, M.; Tschesche, H.; Bode, W.; Gomis-Rueth, F. X. *Eur. J. Biochem.* **1997**, *247*, 356–363.

(24) Gonnella, N. C.; Li, Y.-C.; Zhang, X.; Paris, C. G. *Bioorg. Med. Chem.* **1997**, *5*, 2193–2201.

(25) Moy, F. J.; Chanda, P. K.; Cosmi, S.; Pisano, M. R.; Urbano, C.; Wilhelm, J.; Powers, R. *Biochemistry* **1998**, *37*, 1495–1504.

(26) Moy, F. J.; Chanda, P. K.; Chen, J. M.; Cosmi, S.; Edris, W.; Skotnicki, J. S.; Wilhelm, J.; Powers, R. *Biochemistry* **1999**, *38*, 7085–7096.

(27) Hajduk, P. J.; Sheppard, G.; Nettlesheim, D. G.; Olejniczak, E. J. *J. Am. Chem. Soc.* **1997**, *119*, 5818–5827.

(28) Olejniczak, E. T.; Hajduk, P. J.; Marcotte, P. A.; Nettlesheim J. *Am. Chem. Soc.* **1997**, *119*, 5828–5832.

(29) Weingarten, H.; Feder, J. *Anal. Biochem.* **1985**, *24*, 437–440.

(30) Bickett, D. M.; Green, M. D.; Berman, J.; Dezube, M.; Howe, A. S.; Brown, P. J.; Roth, J. T.; McGeehan, G. M. *Anal. Biochem.* **1993**, *212*, 58–64.

(31) Jarvis, R. A.; Patrick, E. A. *IEEE Trans. Comput.* **1973**, *C-22*, 1025–1034.

(32) Denzoi, F.; Lang, R. *J. Immunol. Methods* **1986**, *89*, 271–277.

(33) Martin, E. J.; Critchlow, R. E.; Spellmeyer, D. C.; Rosenberg, S.; Spear, K. L.; Blaney, J. M. *Pharmacol. Libr.* **1998**, *29*, 133–146.

The organics were combined, washed with water and brine, dried over Na_2SO_4 , and concentrated in vacuo to provide an oil that was purified via column chromatography using hexane/ethyl acetate (1:1) followed by $\text{CHCl}_3/\text{MeOH}$ (95:5) as eluant to yield 253 mg (58%) of the desired product as a white solid. Mp 90–94 °C. ^1H NMR (400 MHz, $\text{DMSO}-d_6$) δ 1.46 (s, 3 H), 2.25 (s, 3 H), 3.70 (q, $J = 5.72$ Hz, 2 H), 4.23 (t, $J = 5.74$ Hz, 2 H), 4.62 (d, $J = 14.2$ Hz, 1 H), 5.02 (d, $J = 14.2$ Hz, 1 H), 7.05–7.80 (comp m, 16 H), 9.00 (t, $J = 5.64$ Hz, 1 H), 12.70 (s, 1 H). High-resolution mass spectra (ESI) m/z 599.18424 [(M + H)⁺ C₃₃H₃₁N₂O₇S requires 599.18465].

Benzofuran-2-carboxylic acid (2-[4-[benzyl-(2-hydroxycarbonyl)-4,6-dimethylphenyl)sulfamoyl]phenoxy]ethyl)amide (WAY-170523): Acid 13 (170 mg, 0.28 mmol) was dissolved in DMF (5 mL). To this was added hydroxybenzotriazole (92 mg, 0.68 mmol) followed by 1-(3-dimethylaminopropyl)-3-ethylcarbodiimide hydrochloride (150 mg, 0.78 mmol). The reaction was stirred for 1 h and then hydroxylamine hydrochloride (156 mg, 2.24 mmol) and triethylamine (0.39 mL, 2.8 mmol) were added and the resulting mixture was stirred overnight. The reaction was then diluted with CH_2Cl_2 and washed with water, 1 M HCl, NaHCO_3 (saturated), and brine, dried over Na_2SO_4 , and concentrated in vacuo to provide an oil that was triturated with ether to provide the desired hydroxamic acid as a beige solid (58% yield). IR (KBr) 3380, 1653, 1595, 1496, 1257, 1153, 1093, 853, 750, 700 cm^{-1} . ^1H NMR (400 MHz, $\text{DMSO}-d_6$) δ 1.54 (s, 3 H), 2.25 (s, 3 H), 3.70 (q, $J = 5.7$ Hz, 2 H), 4.25 (t, $J = 5.8$ Hz, 2 H), 4.73 (d, $J = 2$ Hz, 2 H), 6.98 (d, $J = 5.72$ Hz, 2 H), 7.07–7.24 (comp m, 4 H), 7.41 (dt, $J = 7.4$, 5.2 Hz, 2 H), 7.58 (d, $J = 0.68$ Hz, 1 H), 7.66 (d, $J = 8.4$ Hz, 1 H), 7.79 (m, 2 H), 8.83 (t, $J = 2.5$ Hz, 1 H), 8.97 (t, $J = 5.6$ Hz, 1 H). High-resolution mass spectra (ESI) m/z 614.19532 [(M + H)⁺ C₃₃H₃₂N₃O₇S requires 614.19555].

NMR Sample Preparation. Uniformly (>95%) ^{15}N - and $^{15}\text{N}/^{13}\text{C}$ -labeled human recombinant MMP-13 was expressed in *E. coli* and purified as described previously.^{9,34} 1 mM $^{13}\text{C}/^{15}\text{N}$ - and ^{15}N -MMP-13 NMR samples were prepared by concentration and buffer exchange using Millipore Ultrafree-10 centrifugal filters into a buffer containing 10 mM deuterated Tris-base, 100 mM NaCl, 5 mM CaCl_2 , 0.1 mM ZnCl_2 , 2 mM NaN_3 , and 10 mM deuterated DTT in 90% $\text{H}_2\text{O}/10\%$ D_2O or 100% D_2O . The 10:1 CL-82198:MMP-13 samples were prepared by addition of CL-82198 into either a 1 mM $^{13}\text{C}/^{15}\text{N}$ - or ^{15}N -MMP-13 sample followed by pH readjustment. The sample to explore the potential of competitive inhibition between CL-82198 and WAY-151693 was prepared by first adding 1 mM WAY-151693 to a 1 mM ^{15}N -MMP-13 sample followed by the addition of 10 mM CL-82198. The initial MMP-13:WAY-151693 sample was made by buffer exchange of ^{15}N -MMP-13 into the buffer containing 0.1 mM WAY-151693 followed by additional buffer exchanges to remove excess WAY-151693. Finally, 10 mM of CL-82198 was added to the 1 mM ^{15}N -MMP-13:WAY-151693 sample followed by pH readjustment.

NMR Data Collection. All spectra were recorded at 35 °C on a Bruker AMX-2 600 spectrometer using a gradient enhanced triple-resonance $^1\text{H}/^{13}\text{C}/^{15}\text{N}$ probe. For spectra recorded in H_2O , water suppression was achieved with the WATERGATE sequence and water-flip back pulses.^{35,36} Quadrature detection in the indirectly detected dimensions was recorded with a States-TPPI hypercomplex phase increment.³⁷ Spectra were collected with appropriate refocusing delays to allow for 0,0 or -90,180 phase correction.

Spectra were processed using the NMRPipe software package³⁸ and analyzed with PIPP³⁹ on a Sun Ultra10 Workstation. When appropriate, data processing included a solvent filter, zero-padding data to a power of 2, linear prediction back one data point of indirectly acquired data to obtain zero phase corrections, and linear prediction of additional

points for the indirectly acquired dimensions to increase resolution. Linear prediction by the means of the mirror image technique was used only for constant-time experiments.⁴⁰ In all cases data were processed with a skewed sine-bell apodization function and one zero-filling was used in all dimensions.

The general approach for determining the structure of CL-82198 bound to MMP-13 based on a previously solved NMR structure was described in detail previously.²⁶

The resonance assignments and bound conformation of CL-82198 in the MMP-13:CL-82198 complex were based on the 2D $^{12}\text{C}/^{12}\text{C}$ -filtered NOESY,^{41,42} 2D $^{12}\text{C}/^{12}\text{C}$ -filtered TOCSY,^{41,42} and $^{12}\text{C}/^{12}\text{C}$ -filtered COSY experiments.⁴³

The assignments of the ^1H , ^{15}N , and ^{13}C resonances of MMP-13 in the MMP-13:CL-82198 complex were based on the previous assignments for the MMP-13:WAY-151693 complex³⁴ in combination with a minimal set of experiments: 2D ^1H - ^{15}N HSQC, 3D ^{15}N -edited NOESY,^{44,45} CBCA(CO)NH,⁴⁶ C(CO)NH,⁴⁷ HNHA,⁴⁸ and HNCA.⁴⁹

The MMP-13:CL-82198 structure is based on observed NOEs from the 3D ^{15}N -edited NOESY^{44,45} and 3D ^{13}C -edited/ ^{12}C -filtered NOESY.^{50,48} The 3D ^{15}N -edited NOESY and 3D ^{13}C -edited/ ^{12}C -filtered NOESY experiments were collected with 100 and 110 ms mixing times, respectively. The acquisition parameters for each of the experiments used in determining the solution structure of the MMP-13:CL-82198 complex were as reported previously.^{26,51} As a result of the weak binding affinity of CL-82198 with MMP-13 only a minimal number of intermolecular NOEs were observed. The number of observed NOEs was insufficient for a detailed simulated annealing approach for solving the structure of the MMP-13:CL-82198 complex, but was sufficient for validating a minimized docked model of the complex.

Molecular Analysis and Design. The minimized models of CL-82198 and WAY-152177 complexed to MMP-13 were prepared as previously described.^{52,53} Using molecular dynamics methods (Sybyl v6.4 from Tripos Inc), protein regions within 5 Å from CL-82198 were sampled along with the inhibitor, whereas everything else remained rigid during the simulations. Upon energy convergence, the last 50 frames from the final 100-ps run were averaged and this averaged structure underwent a final minimization. The final MMP-13:CL-82198 model appeared to have optimized possible polar and van der Waals interactions (Figure 4B). Validity of the final MMP-13:CL-82198 model was determined by consistency with the experimental NOEs observed for the complex. The identical procedure was applied to the complex of MMP-13 and WAY-152177 (experimental structure not shown). Since the two complexes used identical MMP-13 structures, the proteins were overlapped to depict the positions of the two inhibitors within the active site. Graphics analysis of the inhibitors showed that the methylene carbon of CL-82198 containing the 2HB1/2 protons (Figure 2) overlapped identically with the methoxy carbon from WAY-152177. This analysis indicated the optimal or minimal linkage length required to connect the benzofuran moiety to the methoxy region of WAY-152177. The final design scheme is shown in Figure 6 for the hybrid

(40) Zhu, G.; Bax, A. *J. Magn. Reson.* **1992**, *100*, 202–7.

(41) Petros, A. M.; Kawai, M.; Luly, J. R.; Fesik, S. W. *FEBS Lett.* **1992**, *308*, 309–14.

(42) Gemmecker, G.; Olejniczak, E. T.; Fesik, S. W. *J. Magn. Reson.* **1992**, *96*, 199–204.

(43) Ikura, M.; Bax, A. *J. Am. Chem. Soc.* **1992**, *114*, 2433–40.

(44) Marion, D.; Driscoll, P. C.; Kay, L. E.; Wingfield, P. T.; Bax, A.; Gronenborn, A. M.; Clore, G. M. *Biochemistry* **1989**, *28*, 6150–6.

(45) Zuiderweg, E. R. P.; Fesik, S. W. *Biochemistry* **1989**, *28*, 2387–91.

(46) Grzesiek, S.; Bax, A. *J. Am. Chem. Soc.* **1992**, *114*, 6291–3.

(47) Grzesiek, S.; Anglister, J.; Bax, A. *J. Magn. Reson., Ser. B* **1993**, *101*, 114–19.

(48) Vuister, G. W.; Bax, A. *J. Am. Chem. Soc.* **1993**, *115*, 7772–7.

(49) Kay, L. E.; Ikura, M.; Tschudin, R.; Bax, A. *J. Magn. Reson.* **1990**, *89*, 496–514.

(50) Lee, W.; Revington, M. J.; Arrowsmith, C.; Kay, L. E. *FEBS Lett.* **1994**, *350*, 87–90.

(51) Moy, F. J.; Seddon, A. P.; Boehlen, P.; Powers, R. *Biochemistry* **1996**, *35*, 13552–13561.

(52) Chen, J. M.; Sheldon, A.; Pincus, M. R. *J. Biomol. Struct. Dyn.* **1995**, *12*, 1129–1159.

(53) Chen, J. M.; Xu, S. L.; Wawrzak, Z.; Basarab, G. S.; Jordan, D. B. *Biochemistry* **1998**, in press.

(34) Moy, F. J.; Chanda, P., K.; Cosmi, S.; Edris, W.; Levin, J. I.; Powers, R. *J. Biomol. NMR* **2000**, in press.

(35) Piotto, M.; Saudek, V.; Sklenar, V. *J. Biomol. NMR* **1992**, *2*, 661–5.

(36) Grzesiek, S.; Bax, A. *J. Am. Chem. Soc.* **1993**, *115*, 12593–4.

(37) Marion, D.; Ikura, M.; Tschudin, R.; Bax, A. *J. Magn. Reson.* **1989**, *85*, 393–9.

(38) Delaglio, F.; Grzesiek, S.; Vuister, G. W.; Zhu, G.; Pfeifer, J.; Bax, A. *J. Biomol. NMR* **1995**, *6*, 277–293.

(39) Garrett, D. S.; Powers, R.; Gronenborn, A. M.; Clore, G. M. *J. Magn. Reson.* **1991**, *95*, 214–20.

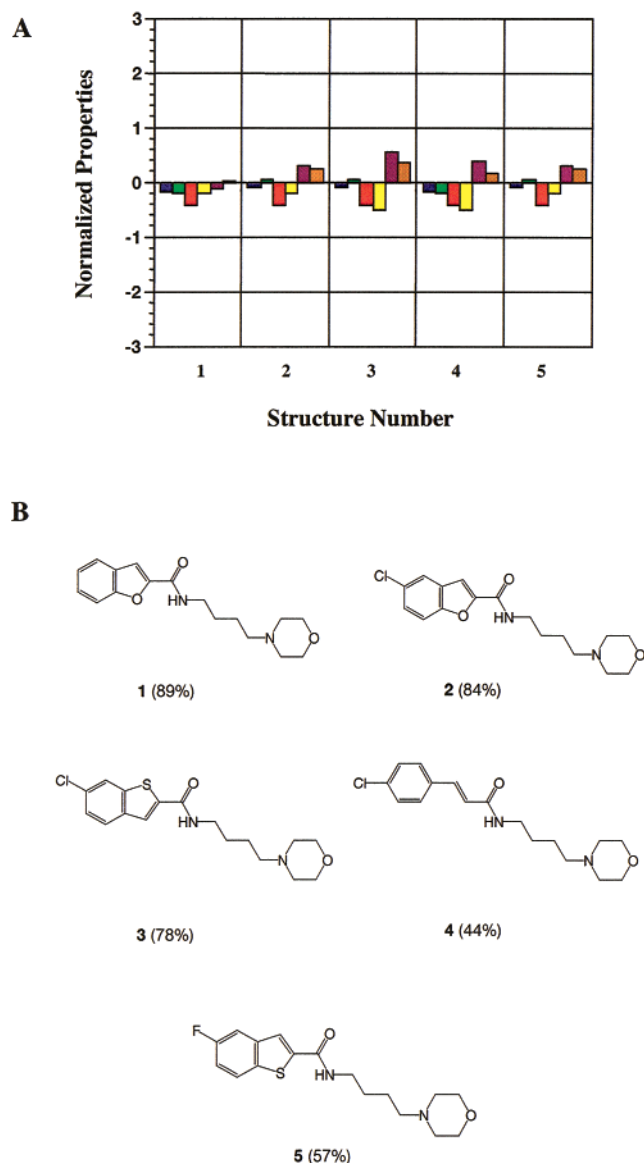


Figure 1. (A) A column graph depicting the normalized property values for each structure in the cluster. For each compound the normalized values of the six properties are shown by different colored columns: total number of non-hydrogen atoms (blue); number of heteroatoms (green); number of hydrogen-bond donors (red); number of hydrogen-bond acceptors (yellow); calculated log *P* (purple); and molecular weight (orange). The profiles for the five different compounds are arrayed next to each other. Note that every compound in the cluster deviates less than 1 standard deviation from the mean value for the marketed drugs in respect to each of the six properties. The mean values for the marketed drugs are as follows: total number of non-hydrogen atoms (25); number of heteroatoms (6.9); number of hydrogen-bond donors (1.8); number of hydrogen-bond acceptors (4.7); calculated log *P* (2.2); and molecular weight (335). (B) The structures of the five compounds comprising the cluster. The values in parentheses are the percent inhibition values measured in the MMP-13 inhibition assay. CL-82198 is labeled as compound **1** in the cluster.

inhibitor. The homology model of MMP-9 was constructed using the COMPOSER program (Tripos INC, Sybyl v.6.4).

Results and Discussion

High Throughput Screening Analysis. CL-82198 was identified as an initial lead from the analysis of the MMP-13 high throughput screen (HTS). A total of 385 compounds from the 58079 compounds screened were identified as MMP-13

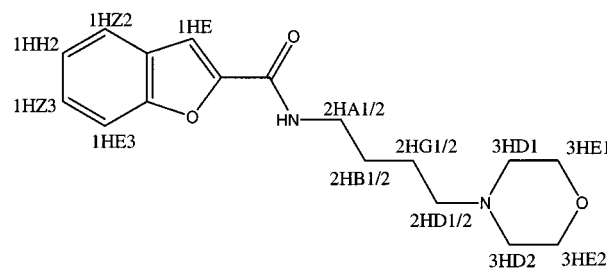


Figure 2. Illustration of the CL-82198 inhibitor with the corresponding proton labels.

inhibitors but only 223 of the 385 hits were identified as viable synthetic targets. The 223 hits were clustered based on structural similarities and the properties of these compounds were compared against the properties of the set of orally available drugs. This profile analysis provides an initial means to predict the likelihood that an HTS hit may have the characteristics of an orally bioavailable drug. Using these criteria, the cluster containing CL-82198 was identified for further analysis. The normalized property profile for this cluster is shown in Figure 1A and the corresponding structures for the cluster are shown in Figure 1B. It is clear from Figure 1 that none of the five compounds in the cluster exhibit significant deviations in physical properties relative to the set of orally available drugs. Also, it is apparent that members of the cluster are close structural analogues suggesting a structure–activity relationship. These results identified this cluster as a possible source of a potentially new series of MMP-13 inhibitors. CL-82198 (compound 1) was shown to exhibit weak inhibition of MMP-13 (89% at the 10 $\mu\text{g}/\text{mL}$), but more intriguing was the observation of a complete lack of activity against other MMPs (MMP-1, MMP-9, and TACE). The profile of CL-82198 illustrated in Figure 1A indicates that the compound has properties similar to orally available drugs suggesting that it would be an ideal candidate for optimization of its enzyme potency and selectivity. The primary structure of CL-82198 along with the proton naming convention is shown in Figure 2. A common feature of known MMP inhibitor structures is the presence of a Zn-chelator that plays a fundamental role in its activity. In most cases Zn chelation occurs from the presence of a hydroxamic acid in the structure of the small molecule. As apparent from the structure of CL-82198 (Figure 2), the compound does not contain an obvious substituent that would chelate Zn. Thus, the unique structure of CL-82198 suggested a potential novel mechanism for inhibition of MMP-13 further strengthening the choice of CL-82198 as an initial lead candidate. Therefore, the identification of CL-82198 as a candidate to optimize its activity and selectivity was based on three unique observations: its intrinsic MMP-13 selectivity, its structural profile similar to known bioavailable drugs, and finally its apparent novel structure.

NMR Structure of the MMP-13:CL-82198 Complex. The NMR binding studies provided critical information pertaining to the mechanism of CL-82198 inhibition of MMP-13 and the method for designing increased potency. The major question presented when CL-82198 was identified from HTS was its unknown MMP-13 binding site and its method for inducing MMP-13 inhibition. Our previous work on the NMR structure of MMP-13 complexed with WAY-151693 and MMP-1 complexed with CGS-27023A provided the framework and methodology to analyze CL-82198 bound to MMP-13.^{9,26}

The CL-82198 MMP-13 binding site was initially identified from chemical shift perturbation in the ^1H – ^{15}N HSQC spectra. The observed perturbations were mapped onto a GRASP surface as depicted in Figure 3. It is apparent that the major effect of

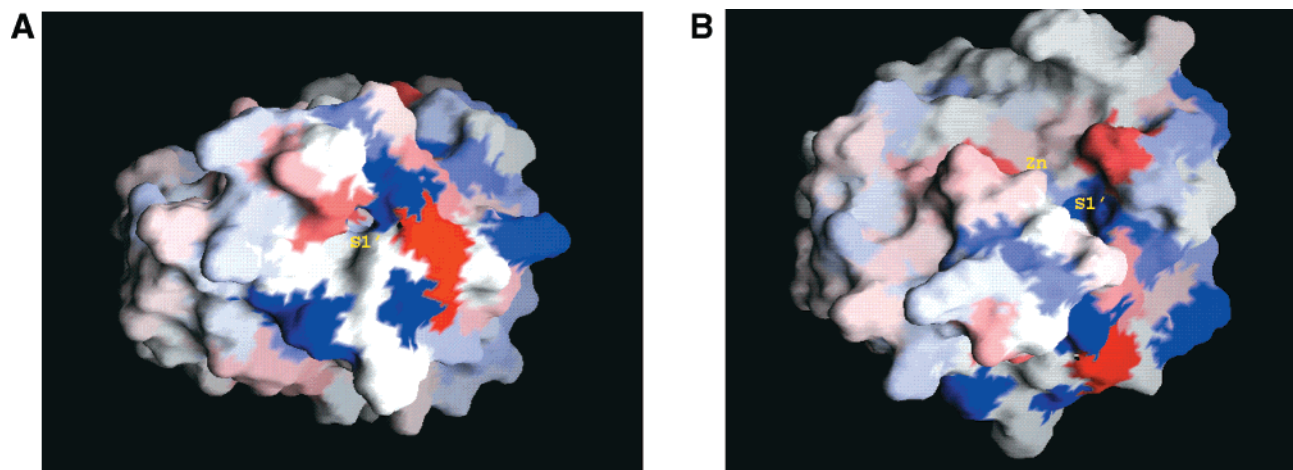


Figure 3. Two GRASP surface views for MMP-13 colored by the observed chemical shift perturbation induced by the binding of CL-82198: (A) looking down the S1' binding pocket and (B) the base of the S1' binding pocket. Red corresponds to a negative chemical shift change and blue corresponds to a positive chemical shift change.

CL-82198 on the chemical shifts of MMP-13 occurs in the proximity of the S1' pocket suggesting that CL-82198 sits in this pocket. From the NMR and X-ray structures of MMP-13, it was determined that the S1' pocket for MMP-13 is very deep and linear in shape while nearly reaching the surface of the protein. In fact, a number of residues at the surface of MMP-13 near the base of the S1' pocket show significant chemical shift perturbation in the presence of CL-82198. Since CL-82198 is a linear molecule, docking studies would place the inhibitor stretched throughout the linear S1' pocket of MMP-13. The only question remaining was whether to place the morpholine or the benzofuran moiety of CL-82198 at one end of the pocket, adjacent to the catalytic zinc or at the opposite end, distant from the zinc atom. Property analysis of the enzyme's S1' pocket depicts that the end adjacent to the zinc is relatively polar whereas the opposite end is hydrophobic. This analysis led us to dock CL-82198 with the morpholine ring adjacent to the catalytic zinc atom with the benzofuran moiety sitting in a hydrophobic pocket formed by L115, L136, F149, and P152 at the base of the S1' pocket. To further verify the proposed binding of CL-82198 in the S1' pocket of MMP-13, a simple competition experiment with WAY-151693 was conducted. The ^1H - ^{15}N HSQC experiment for the MMP-13:CL-82198 complex was collected in the presence of WAY-151693. The presence of WAY-151693 displaced all of CL-82198 as evident by the distinct differences in the ^1H - ^{15}N HSQC spectra, which further suggests that both compounds bind in the S1' pocket (data not shown).

The relative orientation and binding of CL-82198 with MMP-13 was further confirmed by the observation of intermolecular NOEs between CL-82198 and MMP-13 from the 3D ^{13}C -edited/ ^{12}C -filtered NOESY experiment. The NOESY spectra were collected in the presence of a 10-fold excess of CL-82198 because of the weak affinity of CL-82198 with MMP-13. Nevertheless, a total of 16 NOEs were observed between CL-82198 and L81, L115, V116, Y141, T142, and Y143, which support the initial positioning of CL-82198 in the MMP-13 S1' pocket. An expanded 2D plane from the 3D ^{13}C -edited/ ^{12}C -filtered NOESY experiment is shown in Figure 4A, which demonstrates examples of some key intermolecular NOEs between CL-82198 benzofuran group resonances and L115 δ and CL-82198 resonances proximal to the morpholine ring and L82 δ . The complex of CL-82198 with MMP-13 was subjected to energy refinement using the NMR results as constraints.^{26,52} An expanded view of the refined NMR structure of MMP-13

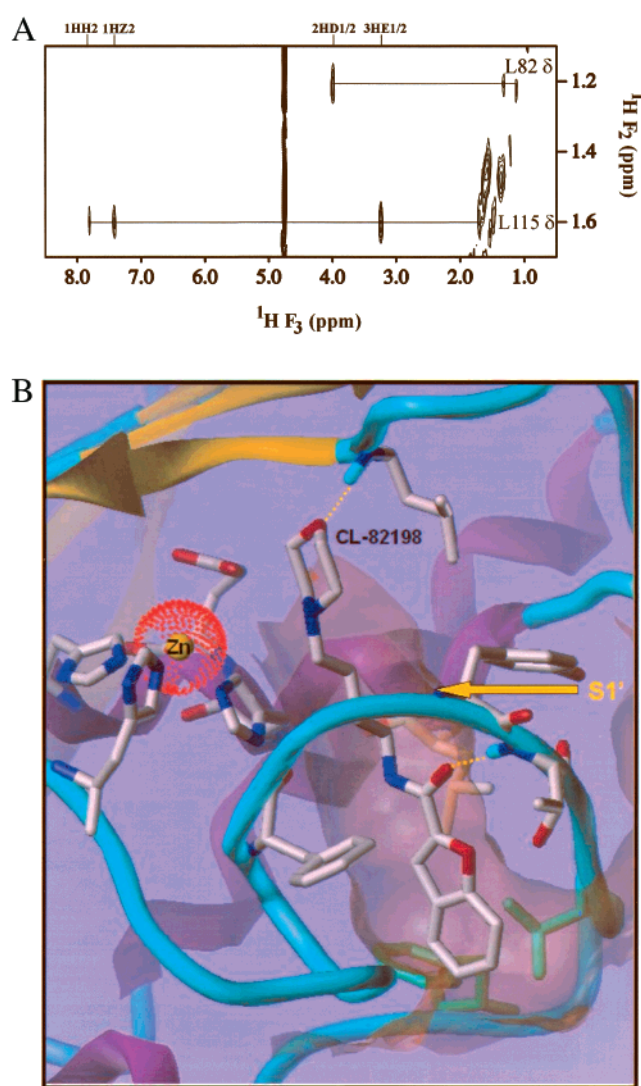


Figure 4. (A) Expanded 2D plane from the 3D ^{13}C -edited/ ^{12}C -filtered NOESY experiment corresponding to NOEs from L82 δ and L115 δ to the labeled resonances from CL-82198. (B) Expanded view of the NMR MMP-13:CL-82198 complex where the MMP-13 active site is shown as a transparent surface with CL-82198 shown as liquorice bonds. View is looking at the S1' pocket.

complexed with CL-82198 is shown in Figure 4B. The modeling results depict the morpholine oxygen forming a hydrogen bond

Table 1. IC50 and Selectivity Data

compd	MMP-1	MMP-9	MMP-13	TACE	S-1 ^a	S-9 ^a	S-TACE ^a
WAY-152177	82 nM	21 nM	15 nM	240 nM	5.5×	1.4×	16×
WAY-159062	750 nM	46 nM	75 nM	470 nM	10.0×	0.6×	6.3×
WAY-159063	1025 nM	71 nM	301 nM	664 nM	3.4×	0.2×	2.2×
WAY-170523	NA (10 μM)	945 nM	17 nM	19% (1 μM)	>5800×	56×	>500×

^a Selectivity data presented as a ratio of the MMP or TACE IC50 with MMP-13. NA, no activity observed at the indicated concentration.

Table 2. Sequence Comparison

position ^a	MMP-1	MMP-9	MMP-13
115	ARG	LEU	LEU
144	VAL	ARG	VAL

^a The residue numbering corresponds to the sequence for the MMP-13 structure.

with the backbone amide group of Leu-82 and the benzofuran group packs deep in the S1' pocket with the peptide bond linker portion forming hydrogen bonds with protein backbone groups. The complex shows no apparent interactions between the inhibitor and the catalytic zinc, justifying the ligands micromolar potency.

Structures of MMP-1, MMP-9, and MMP-13. The recent NMR solution structures of MMP-1 and MMP-13 were used as starting points for molecular modeling and analysis.^{9,25,26} At the start of this study, the experimental structure of MMP-9 was not available, therefore, a model was developed based on its strong homology to MMP-1 (54% identity around the catalytic domain). Overall, the catalytic site of MMP-9 is similar to the corresponding sites in MMP-1 and MMP-13. All three structures were used as starting points for analysis and synthetic design.

Comparative analysis of the MMP structures shows that residue positions 115 and 144 (based on the MMP-13 sequence numbering), in addition to the length of the specificity loop, determine the size and shape of the S1' pockets. Alignment of the NMR structures for MMP-1 and MMP-13 shows that MMP-13 contains two additional insertions in the specificity loop. The homology model of MMP-9 indicates no additional insertions so its length is identical to that of MMP-1.

Residue positions 115 and 144 are important in establishing the relative length of the S1' pockets for the MMPs where the larger side chain at these positions results in a smaller S1' pocket. Since residue 115 is spatially closer to the catalytic zinc than residue 144, a larger side chain for residue 115 will have a greater impact on defining a smaller S1' pocket compared to residue 144. As can be seen in Table 2, MMP-1 has the largest side chain at position 115, thus its S1' pocket is the smallest. MMP-9 has an Arg at position 144 resulting in its S1' pocket being longer compared to MMP-1. Conversely, MMP-13 has short side chains at both positions 115 and 144. The short side chains combined with an increased length of its specificity loop result in MMP-13 having the largest S1' pocket. To summarize, the sizes of the MMP S1' pockets are as follows: MMP-13 > MMP-9 > MMP-1 where this structural feature plays a critical role in the design strategy for developing a potent and specific MMP-13 inhibitor.

Design Strategy. A strategy utilizing NMR and molecular modeling was applied toward the design and synthesis of an MMP-13 selective inhibitor lead. The basic approach behind the design strategy is to optimize the affinity of the chemical lead CL-82198 while maintaining its inherent MMP-13 selectivity. This can be achieved by taking advantage of the distinct structural feature of MMP-13, its deep linear S1' pocket, while combining overlapping structural features of CL-82198 with

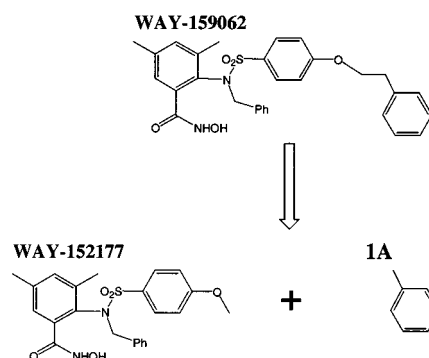


Figure 5. Design scheme dividing WAY-159062 into two components corresponding to its potency component and its selectivity component. Basis for the design of a hybrid with CL-82198.

other potent inhibitors. WAY-159062 is an example of a potent and selective inhibitor for MMP-9 and MMP-13 (see Table 1). Structurally similar inhibitors were positioned into the active site of MMP-13 based on the NMR solution structure of MMP-13 complexed with WAY-151693⁹ and MMP-1 complexed with CGS-27023A.²⁶

Figure 5 shows the critical regions of WAY-159062, which can be broken down into two components, WAY-152177, which represents the zinc chelating portion of the compound that contributes to the binding potency, and the toluene group (1A), which contributes to enhanced ligand selectivity against MMP-1. The strategy was to design a new inhibitor based on replacing the toluene group (1A) with a component of CL-82198 critical for binding within the extended S1' pocket of MMP-13. The overlay of the NMR solution structure for CL-82198 with the model for WAY-152177 is shown in Figure 6B. The close similarity between the positioning of the two structures made it readily apparent that it would be possible to generate a hybrid of the two structures combining the potent WAY-152177 with the selective component of CL-82198 (Figure 6). These results were then used to design the proposed *hybrid inhibitor* WAY-170523 (see Figures 5 and 6). The synthesis of the inhibitor was accomplished in a straightforward manner beginning with the known⁵⁴ acid (**12**) (Scheme 1). Fluoride displacement with the sodium salt of benzofuran alcohol (**11**) (prepared via condensation of benzofuran carboxylic acid with ethanolamine) provided the elaborated acid (**13**). Condensation of the acid with hydroxylamine hydrochloride mediated by hydroxybenzotriazole and 1-(3-dimethylaminopropyl)-3-ethylcarbodiimide hydrochloride then produced the desired hydroxamic acid. When tested against several members of the MMP family, the data in Table 1 clearly show that the new inhibitor, WAY-170523, has better potency compared to WAY-159062 in addition to improved selectivity toward MMP-13. With a proof of concept now demonstrated for establishing selectivity versus MMP-9, this hybrid inhibitor now provides a starting point for the design of potent, selective, orally bioavailable inhibitors of MMP-13. Sulfonamide MMP inhibitors similar to this inhibitor have

(54) Levin, J. I.; Du, M. T.; Venkatesan, A. M.; Nelson, F. C.; Zask, A.; Gu, Y.: United States patent number 5,929,097, 1999.

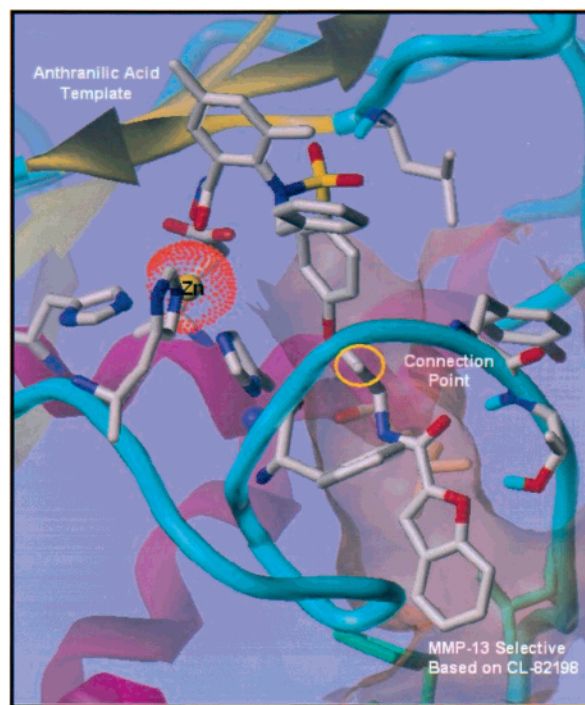
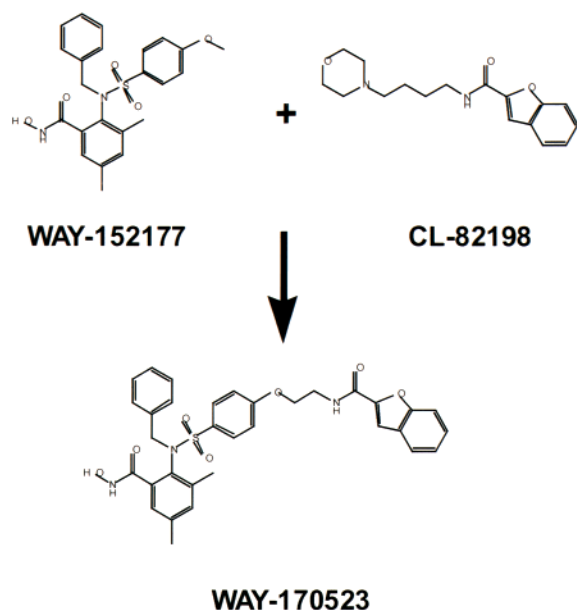
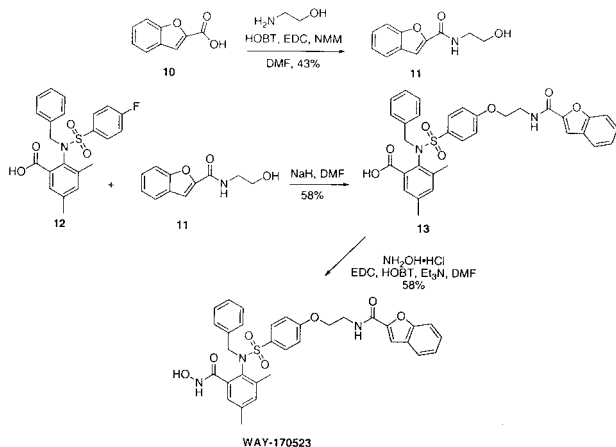


Figure 6. (A) Design scheme showing the flow from CL-82198 and WAY-159062 to WAY-170523. (B) Expanded view of the NMR MMP-13:CL-82198 complex overlaid with the MMP-13:WAY-152177 model demonstrating the approach to forming the hybrid inhibitor WAY-170523 where the MMP-13 active site is shown as a grid surface with CL-82198 and WAY-152177 is shown as liquorice bonds. View is looking at the S1' pocket.

Scheme 1



shown enhanced oral potency when basic amines have been incorporated into the molecule.⁵⁵ Further studies are underway to reach the combined target of selectivity with oral activity.

Conclusion

The extensive structural information available for the MMP family of proteins provided the essential elements for designing

a potent and selective inhibitor for MMP-13. Specifically, these data identified the potential utility of the size, shape and nature of the S1' pocket in designing specificity into MMP inhibitors. Additionally, the abundance of information available on the nature of MMP inhibitors indicated general characteristics that were necessary for inhibitor potency. The NMR structures for MMP-13 and MMP-1 were the initial starting points for a structure-based approach for developing a selective MMP-13 inhibitor. In addition, the structural information for the WAY-151693 and CGS-27023A complexes was critical for adapting design elements into the initial CL-82198 structure, since these complex structures reliably predicted the bound structures of new analogues. Thus, the combination of NMR spectroscopy with molecular modeling techniques and HTS data resulted in the design of a novel, potent, and selective MMP-13 inhibitor (WAY-170523) which has an IC₅₀ of 17 nM for MMP-13 and showed >5800-, 56-, and >500-fold selectivity against MMP-1, MMP-9, and TACE, respectively. To the best of our knowledge, this represents the first example of a potent MMP-13 inhibitor that has been shown to be selective against MMP-9.

Acknowledgment. The authors would like to thank Pranab K. Chanda, Scott Cosmi, Wade Edris, and Jim Wilhelm for providing the MMP samples, Mei-Li Sung, Rebecca Cowling, and Loran M. Killar for providing the IC₅₀ data, Linda Heydt and Fernando Ramirez for providing the high throughput screening results, and Kathryn Bracken and Erin Mattingly for chemical synthesis.

(55) MacPherson, L. J.; Bayburt, E. K.; Capparelli, M. P.; Carroll, B. J.; Goldstein, R.; Justice, M. R.; Zhu, L.; Hu, S.-I.; Melton, R. A.; Fryer, L.; Goldberg, R. L.; Doughty, J. R.; Spirito, S.; Blancuzzi, V.; Wilson, D.; O'Byrne, E. M.; Ganu, V.; Parker, D. T. *J. Med. Chem.* **1997**, *40*, 2525–2532.